THE JOURNAL OF BIOLOGICAL CHEMISTRY VOL. 285, NO. 22, pp. 16467–16475, May 28, 2010

Separate Gating Mechanisms Mediate the Regulation of K_{2P} Potassium Channel TASK-2 by Intra- and Extracellular pH*[S]

Received for publication, January 22, 2010, and in revised form, March 5, 2010 Published, JBC Papers in Press, March 29, 2010, DOI 10.1074/jbc.M110.107060

María Isabel Niemeyer[‡1], L. Pablo Cid[‡], Gaspar Peña-Münzenmayer[‡§], and Francisco V. Sepúlveda[‡¶]

From the [‡]Centro de Estudios Científicos (CECS) and [¶]Centro de Ingeniería de la Innovación Asociado al CECS, Valdivia 5110466, Chile and the [§]Universidad Austral de Chile, Valdivia 5110566, Chile

TASK-2 (KCNK5 or K_{2P}5.1) is a background K^+ channel that is opened by extracellular alkalinization and plays a role in renal bicarbonate reabsorption and central chemoreception. Here, we demonstrate that in addition to its regulation by extracellular protons (pH_o) TASK-2 is gated open by intracellular alkalinization. The following pieces of evidence suggest that the gating process controlled by intracellular pH (pH_i) is independent from that under the command of pH_o. It was not possible to overcome closure by extracellular acidification by means of intracellular alkalinization. The mutant TASK-2-R224A that lacks sensitivity to pH_o had normal pH_i-dependent gating. Increasing extracellular K^+ concentration acid shifts pH_o activity curve of TASK-2 yet did not affect pH_i gating of TASK-2. pH_o modulation of TASK-2 is voltage-dependent, whereas pH_i gating was not altered by membrane potential. These results suggest that pH_o, which controls a selectivity filter external gate, and pH_i act at different gating processes to open and close TASK-2 channels. We speculate that pH_i regulates an inner gate. We demonstrate that neutralization of a lysine residue (Lys^{245}) located at the C-terminal end of transmembrane domain 4 by mutation to alanine abolishes gating by pH_i. We postulate that this lysine acts as an intracellular pH sensor as its mutation to histidine acid-shifts the pH_i-dependence curve of TASK-2 as expected from its lower pK_a. We conclude that intracellular pH, together with pH_o, is a critical determinant of TASK-2 activity and therefore of its physiological function.

The structural class of two-pore, four-transmembrane domains potassium channel family (K_{2P} or KCNK) includes members that sense external changes in proton concentration. The TASK subfamily members TASK-1 and TASK-3, K_{2P}3.1 and K_{2P}9.1, respectively (1), are active at resting potential and are inhibited by extracellular acidification, whereas members of the TALK subfamily TASK-2, TALK-1, and TALK-2 (K_{2P}5.1, K_{2P}16.1, and K_{2P}17.1) are opened by external alkalinization and are only weakly active at physiological pH (2–5). The TREK group of K_{2P} K^+ channels has been shown to be sensitive to the internal concentration of protons: TREK-1 and -2 (K_{2P}2.1 and K_{2P}10.1) are activated, and TRAAK (K_{2P}4.1) is inhibited by internal acidification (6–9). Recently, TREK-1 and TREK-2 have been found to respond also to external proton concentration within the physiological range (10, 11), but, remarkably, although TREK-1 is strongly inhibited by extracellular acidification, TREK-2 is activated by acidification (11).

It is well known that K^+ channels play important roles in epithelial transport processes of electrolytes and nonelectrolytes (12, 13). The reabsorption of HCO_3^- in the kidney proximal tubules, which accounts for up 80% of the filtered load, is an example. Transepithelial flux of HCO_3^- relies on the coordinated action of a luminal Na^+/H^+ exchanger (NHE3), carbonic anhydrases (II and IV) and a basolateral electrogenic Na^+/HCO_3^- cotransporter (NBCe1-A) that shuttles two negative charges per transport cycle. Continued efflux of HCO_3^- will depolarize the cell, thus decreasing the driving force for the process. It has been proposed that concomitant activation of a basolateral K^+ conductance would be required to produce the hyperpolarization necessary to sustaining HCO_3^- transport. A recent study suggests that TASK-2 channels might be responsible for this conductance (14). It was shown that a leak-type current present in mouse cultured proximal tubule cells when HCO_3^- transport is active is not present in cells from a TASK-2 deficient (knock-out) mouse. The mutant mouse displays a reduced arterial blood pressure and a tendency to loose Na^+ in urine and suffers from metabolic acidosis probably through a proximal tubular loss of Na^+ and HCO_3^-. The authors of this work proposed that accumulation of basolateral HCO_3^- would activate basolateral TASK-2 channels by virtue of the ensuing extracellular alkalinization to provide the hyperpolarization needed for continuous cotransporter activity (14). The presence of extracellular and intracellular carbonic anhydrases and the fact that HCO_3^- is an important mobile buffer in the kidney and other cells (15) predict that changes in its flux will have an impact on intracellular pH (pH_i) in the proximal tubule.

We have now found that pH_o-sensitive K^+ channels belonging to the TALK group, opened by alkaline pH_o, are also sensitive to intracellular pH (pH_i). In contrast, acid-sensitive channels TASK-1 and TASK-3 are indifferent to pH_i. In the present work, we explore in some detail the dependence of TASK-2 upon pH_i, clearly separate the effects of extra- and intracellular pH on TASK-2 and identify Lys^{245}, a residue located at the interface between the last transmembrane domain and the beginning of the large C terminus domain, as a possible sensor transducing the effects of pH_i into gating regulation. The strong dependence of TASK-2 on intracellular pH will have to be taken into account when interpreting the possible role of this K^+

* This work was supported by Fondo Nacional de Ciencia y Tecnología Grant 1090478 and Comisión Nacional de Ciencia y Tecnología Grant 24081049. This paper is dedicated to the people who have suffered the ravages of the recent earthquake and tsunami in our country.

[S] The on-line version of this article (available at http://www.jbc.org) contains supplemental Figs. 1–4 and an additional reference.

[1] To whom correspondence should be addressed: Centro de Estudios Científicos, Av. Arturo Prat 514, Valdivia 5110466, Chile. Tel.: 56-63-234542; Fax: 56-63-234517; E-mail: miniemeyer@cecs.cl.

channel in the process of bicarbonate reabsorption in the proximal tubule.

EXPERIMENTAL PROCEDURES

Constructs and Transient Transfections—Mus musculus TASK-2 (GenBank™ accession number AF319542) plasmid was obtained from mouse kidney (16). Human TALK-2 (GenBank™ accession number BC025726) was obtained from the ATCC mammalian gene collection (Manassas, VA). Mouse TASK-1 (GenBank™ accession number AB008537) was obtained from Dr. Donghee Kim and TASK-3 (GenBank™ accession number AF212827) from Dr. Jürgen Daut. All cDNAs were subcloned into the pCR3.1 vector. Transient transfections were done in HEK-293 cells as described previously using CD8 cotransfection to identify effectively transfected cells (17). The CD8 antigen was revealed with microspheres (Dynabeads) coated with an anti-CD8 antigen. Site-directed mutagenesis and chimaera constructions were done by PCR as described previously (17, 18).

Electrophysiological Recordings—Cells were transferred to the stage of an inverted microscope for study, where they were continuously superfused with a bathing solution containing 67.5 mM Na_2SO_4, 4 mM KCl, 1 mM potassium gluconate, 2 mM $CaCl_2$, 1 mM $MgCl_2$, 105 mM sucrose, 10 mM HEPES/Tris, pH 7.5. The high K^+ solution was obtained by equimolar replacement of Na^+ by K^+. The pipette solution contained 8 mM KCl, 132 mM potassium gluconate, 1 mM $MgCl_2$, 10 mM EGTA, 1 mM Na_3ATP, 0.1 mM GTP, 10 mM HEPES, pH 7.4. In experiments to measure the extracellular pH dependence of the currents, HEPES, used for pH 7.0, 7.5, and 8.0 in the bathing medium was replaced with AMPSO,[2] pH 8.5 and 9.0; CAPS, pH 9.5, 10, and 11; or MES, pH 6.5, 6.0, 5.5, and 5.0. All our experiments keep both intra- and extracellular chloride at 10 mM.

Sulfate was replaced by gluconate in the bath solutions when changes in intracellular pH were required: 135 mM sodium gluconate, 1 mM potassium gluconate, 4 mM KCl, 2 mM $CaCl_2$, 1 mM $MgCl_2$, 105 mM sucrose, 10 mM, HEPES/Tris, pH 7.5. For manipulations with NH_4Cl, NH_4Cl was added as an aliquot from a 2.5 M stock. Solutions containing 33 mM HCO^-_3 were made using the sodium salt with an equivalent decrease in sodium gluconate. This solution was maintained in an atmosphere of 5% CO_2 until used.

In experiments designed to measure the intracellular pH dependence of the currents, we used an approach relying on intracellular loading with a weak base or acid in the pipette solution, which provides a means for imposing and maintaining a chosen pH_i, or, by changing the external concentration of the weak electrolyte, to change pH_i rapidly and reversibly. This procedure has been validated in various cell types by direct measurement of intracellular pH (19, 20). In addition, it has been demonstrated not to be affected by membrane potential in neurons (21). The solutions used here to clamp pH_i are based on those described previously (20). Varying the transmembrane concentration gradient for acetate pH_i was changed according to the relationship:

$$pH_i = pH_o - \log([acetate^-]_o/[acetate^-]_i) \quad \text{(Eq. 1)}$$

The composition of solutions used was as follows: pipette: 82 mM potassium gluconate, 50 mM potassium acetate, 8 mM KCl, 1 mM $MgCl_2$, 10 mM HEPES, 10 mM BAPTA-sodium, pH adjusted to 7.4 with Tris; bath: sodium gluconate *X*, sodium acetate *Y* (where $X + Y = 135$), 4 mM KCl, 4 1 mM potassium gluconate, 2 mM $CaCl_2$, 1 mM $MgCl_2$, 20 mM HEPES, and titrated to pH 7.4 with Tris. The extracellular concentration of acetate was varied between 126 and 1.26 mM to achieve intracellular pH values between 7.0 and 9.0 (20). Intracellular pH values in the range 6.3–8.5 were obtained with a pipette solution containing 10 mM acetate and extracellular acetate concentrations between 125 and 0.8 mM. For pH_i values 7.5–9.5, intracellular acetate was 130 mM, and extracellular acetate varied between 103 and 1.03 mM. Different intracellular acetate concentrations were compensated by equimolar changes in gluconate. Enough sucrose was added to give an osmolality of 300 mosM. When appropriate, Na^+ was replaced by K^+ to achieve symmetrical concentration of potassium.

Standard whole-cell patch clamp recordings were performed as described elsewhere (13, 18). Currents were measured at several potentials, but data mostly reported are those obtained at 0 mV. Recordings of single channels in the inside-out configuration were performed in symmetrical 140 mM K^+. The inside aspect of the patch was bathed with the solution described above for the pipette in whole-cell recording experiments. All chemicals were from Sigma.

Calculations—The effect of pH on currents was evaluated by plotting current (*I*) measured at a membrane potential of 0 mV, against extracellular $[H^+]$. For graphical representation, average ± S.E. I/I_{max} or $I/I_{pH7.5}$ values were obtained from individual experiments. When appropriate, the fit of a Hill equation to the data was done for each individual experiment. The parameters are defined in the following equation: $I = I_{min} + (I_{max} - I_{min})/(1 + ([H^+]/K_{½})^{nH})$. Fits were done using the Marquardt-Levenberg algorithm as implemented in the SigmaPlot software.

RESULTS

Cytosolic pH Regulates TALK-type but Not TASK-type K^+ Channels—Transient transfection of HEK-293 cells with TASK-2 or -3 or with TALK-2 cDNAs results in the generation of K^+ currents as measured in the whole-cell configuration mode of the patch clamp technique. Fig. 1*A* shows currents elicited by pulsing to 0 mV in cells held at −70 mV. The currents are carried by K^+ as intra- and extracellular Cl^- concentrations are made equal (see "Experimental Procedures" for details of solution composition). Measured reversal potential of around −80 mV corresponds well with that of a K^+ current, given K^+ extra-/intracellular concentration ratio of 5/140 mM, and shifts to 0 mV in symmetrical K^+ solutions. When cells are exposed to the weak base NH_4Cl, transmembrane influx of NH_3 leads to rapid rise of pH_i, as intracellular NH_3 combines with protons forming NH^+_4 (22). When this treatment was applied

[2] The abbreviations used are: AMPSO, *N*-(1,1,-dimethyl-2-hydroxyethyl)-3-amino-2-hydroxypropanesulfonic acid; CAPS, 3-(cyclohexylamino)-1-propanesulfonic acid; MES, 2-(*N*-morpholino)ethanesulfonic acid; WT, wild-type; BAPTA, 1,2-bis(2-aminophenoxy)ethane-*N*,*N*,*N*′,*N*′-tetraacetic acid; TM4, transmembrane domain 4.

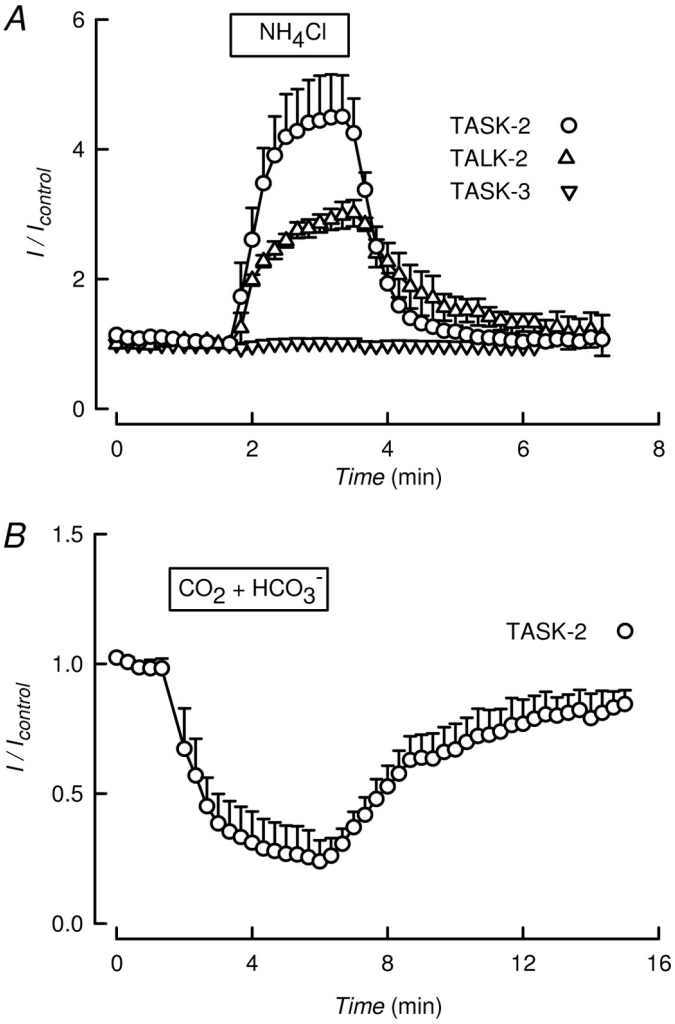

FIGURE 1. **TALK-type K^+ channels are sensitive to intracellular pH.** *A*, K^+ current recorded at 0 mV in HEK-293 cells expressing K_{2P} channels TASK-2, TALK-2, or TASK-3. During the time indicated the solution bathing the cells was switched to one containing 10 mM NH_4Cl. Results are means ± S.E. of six, three, and three experiments, respectively for TASK-2, TALK-2, and TASK-3. *B*, a similar experiment as in *A* but using only TASK-2 and a solution saturated with 5% CO_2 and containing 33 mM HCO_3^-. Means ± S.E. of eight experiments.

to cells expressing TASK-2 or TALK-2 an immediate increase in K^+ current occurred, which reverted to control values upon removal of NH_4Cl (Fig. 1*A*), suggesting that they are activated by intracellular alkalinization. The same procedure caused no change in the K^+ channel activity in cells expressing TASK-3 (Fig. 1*A*) or TASK-1 (data not shown). These channels have previously been shown to be indifferent to internal proton concentration (3, 5, 23). In addition to being activated by intracellular alkalinization, TASK-2 current was inhibited by an acidification of the intracellular medium. This was achieved by a short pulse of a 5% CO_2-HCO_3^- that, owing to the high permeability of CO_2, will rapidly acidify intracellularly. As shown in Fig. 1*B*, such a treatment strongly inhibited the TASK-2-mediated K^+ current. From these qualitative experiments, it would appear that TASK-2 is sensitive to pH_i, being activated by alkalinization and inhibited by acidification.

Internal and External pH Regulation of the TASK-2 Channel Are Independent of Each Other—Yuan *et al.* (20) established that using a 50 mM intracellular acetate concentration and BAPTA to buffer Ca^{2+}, changes in extracellular acetate bring about the expected changes in pH_i as verified by direct measurement with the fluorescent pH probe 2′,7′-bis(2-carboxyethyl)-5(6)-carboxyfluorescein. We have used this acetate-rich pipette to explore in more detail the dependence of TASK-2 activity on pH_i. The use of these solutions did not alter the characteristic open rectification of TASK-2 or its selectivity of K^+ over Na^+ (supplemental Fig. 1). Fig. 2*A* shows the effect of clamping pH_i at values between 7.0 and 9.0 by changing $[acetate^-]_o$ between 1.26 and 126 mM with $[acetate^-]_i$ of 50 mM. TASK-2-mediated current was inhibited by acidification to pH_i 7.0 and was gradually increased by alkalinization. The effect was reversible upon return to a basal pH_i of 7.5.

TASK-2 is gated open by extracellular alkalinization in a similar pH range as described here for intracellular alkalinization. This gating process is mediated by arginine 224, so that mutant TASK-2-R224A channels lack sensitivity to pH_o (24). However, when TASK-2-R224A was challenged with changes in intracellular pH, it was inhibited by intracellular acidification and activated by an alkaline pH_i in much the same way as wild-type (WT) TASK-2 (Fig. 2*B*). Data from six experiments of each WT TASK-2 and TASK-2-R224A at pH_i 7.5 and 9.0 are shown in the right-hand side graphs to Fig. 2, *A* and *B*, and show significant increases in currents measured at 0 mV upon alkalinization from 7.0 to 9.0. Fits of a Hill equation to WT TASK-2 data at 0 mV gave average $pK_{½}$ and n_H values of 8.0 ± 0.07 and 0.9 ± 0.04 ($n = 7$). Equivalent figures for TASK-2-R224A were 7.7 ± 0.22 and 0.9 ± 0.16 ($n = 5$). In Fig. 2*C*, experiments investigating the effect of changes in pH_i at various membrane potentials are shown. The values have been normalized to the currents at pH_i 7.5 and indicate that the membrane potential has no effect on the pH_i sensitivity of TASK-2. This is different from what has been observed for the effect of pH_o on TASK-2, whose $pK_{½}$ shows an acid shift with depolarization (2) (see also Fig. 3*C* below).

In a previous study, we used molecular simulation and site-directed mutagenesis experiments to show that the activation of TASK-2 by extracellular pH is mediated by neutralization of an arginine (Arg^{224}) residue (24). Arg^{224} is located at the extracellular end of TM4 near the second pore domain. The protonated form of Arg^{224} is thought to interfere, through an electrostatic effect, with potassium occupancy of the selectivity filter leading to blockade by a mechanism similar to C-type inactivation (24). This type of inhibition has been shown to be very dependent upon extracellular potassium concentration, which, through a "foot in the door" mechanism, prevents the conformational changes responsible for C-type inactivation (25). We have tested the effect of increasing extracellular K^+ concentration to 140 mM on the modulation of TASK-2 by pH_i. Fig. 3*A* shows that pH_i dependence of TASK-2 was unaffected by increasing extracellular K^+ from 5 to 140 mM. At this high K^+ concentration, the effect of pH_i was also voltage-independent in the range −60 to 60 mV (Fig. 3*A*). This contrasts with the activation of TASK-2 by extracellular pH, which occurred with $pK_{½}$ values for activation of 8.1 and 7.6 at extracellular $[K^+]_o$ of 5 and 140 mM, respectively (Fig. 3*B*). The lack of dependence of the pH_i effect on membrane potential is also in

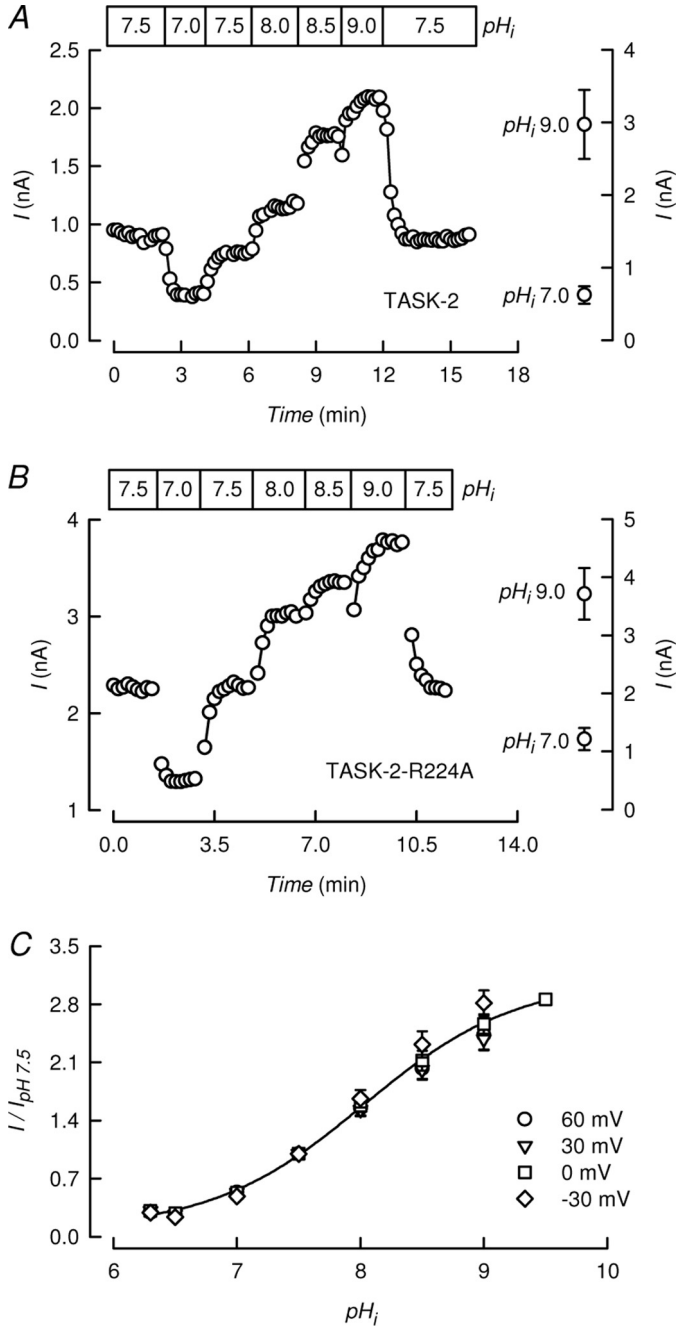

FIGURE 2. **Lack of effect of disabling the extracellular pH sensor and of voltage on TASK-2-mediated currents.** *A*, time course of TASK-2-mediated current recorded at 0 mV at various indicated intracellular pH values. These were achieved in cells containing 50 mM acetate and extracellular acetate concentrations ranging from 1.26 to 126 mM to yield pH_i values ranging from 7.0 to 9.0 (as described under "Experimental Procedures"). On the *right*, average ± S.E. values at pH_i 9.0 and 7.0 ($n = 7$) are reported. Extracellular pH was 7.4 throughout. *B*, an experiment performed as in *A* but using TASK-2-R224A pH_o-insensitive mutant. Average values shown on the *right* are from six experiments. *C*, pH_i dependence of TASK-2 at different voltages (means ± S.E., $n = 4–8$). Extracellular and intracellular K^+ concentrations were 5 and 140 mM, respectively, in *A–C*. The line shows a fit of a Hill function to the data at 0 mV.

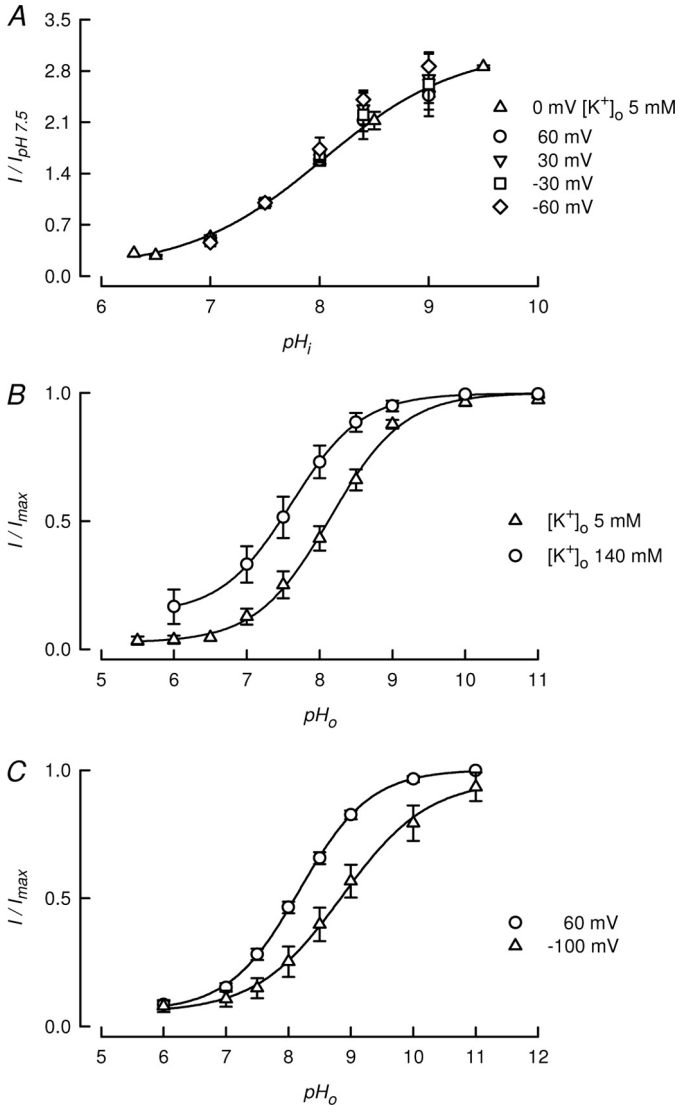

FIGURE 3. **TASK-2 gating by intracellular pH is independent on extracellular K^+ concentration and voltage.** *A*, pH_i dependence of TASK-2 first measured at a $[K^+]_o$ of 5 mM at 0 mV (*triangles*) and then at 140 mM $[K^+]_o$ at voltages from −60 to 60 mV as indicated. Values, normalized to measurements at pH_i 7.5, are means ± S.E. ($n = 3–8$). Extracellular pH was 7.4 throughout. *B*, effect of $[K^+]_o$ on the pH_o dependence of TASK-2. To obtain approximately similar driving forces, measurements were taken at −20 and 60 mV at $[K^+]_o$ 5 and 140 mM, respectively (means ± S.E., of $n = 6$ and 8, respectively). *C*, effect of voltage on the pH_o dependence of TASK-2. Measurements (means ± S.E., $n = 11$) were taken at −100 and 60 mV using $[K^+]_o$ 5 mM. Intracellular K^+ was 140 mM in *A–C*.

contrast with the voltage dependence of the pH_o effect (Fig. 3*C*). Interestingly, this last effect was only observed at low $[K^+]_o$.[3]

The results shown above suggest that gating by extra- and intracellular pH are separate and independent events that must be mediated by distinct molecular sensors and are transduced through actions at gates with different locations. The experiment shown in Fig. 4 is an attempt at overcoming closure by extracellular acidification by means of intracellular alkalinization. Maintaining $[acetate^-]_i$ at 50 mM, we simultaneously changed pH_o and pH_i to obtain a closed channel at pH_o 6.0 and pH_i 7.5, which could not be opened by an increase in pH_i to 8.5 (Fig. 4*A*). In the same cell, the channel was further activated by pH_i 8.5 when the channel was open at a permissive pH_o of 7.93. A bar chart (Fig. 4*B*) summarizes the activation of TASK-2 channel by an increase in pH_i from 7.5 to 8.5 at extracellular pH

[3] M. I. Niemeyer, L. P. Cid, and F. V. Sepúlveda, unpublished data.

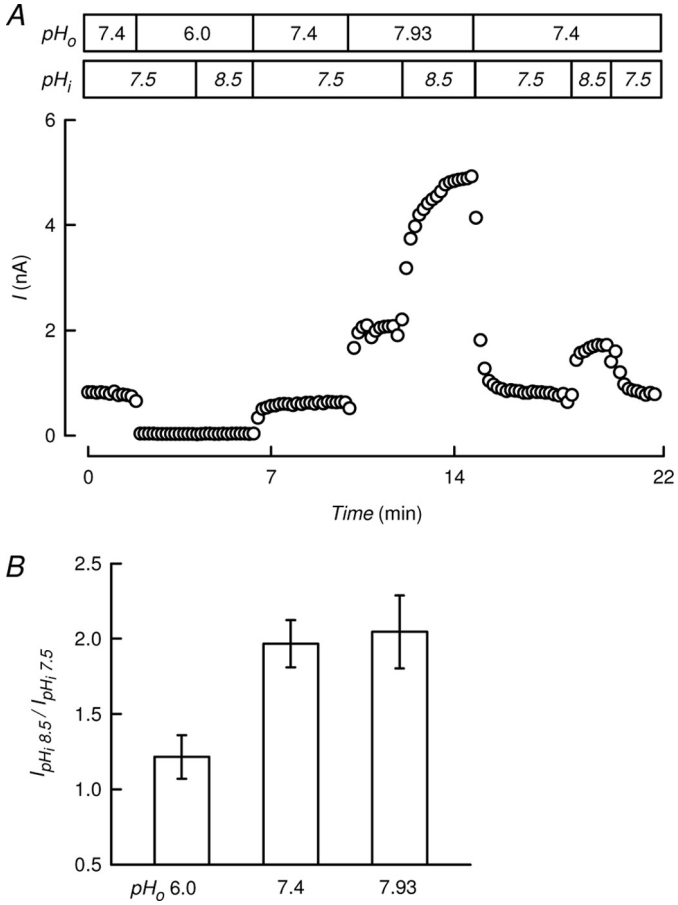

FIGURE 4. **Closure of TASK-2 channels by extracellular acidification cannot be overcome by intracellular alkalinization.** *A*, continuous recording of TASK-2-mediated current using an intracellular acetate concentration of 50 mM and changing extracellular acetate concentration to simultaneously change pH_o and pH_i as indicated. *B*, bar chart summarizing the normalized activation of TASK-2 channel by an increase in pH_i from 7.5 to 8.5 at extracellular pH of 6.0, 7.4, and 7.9. Means ± S.E., $n = 3–9$. Extracellular and intracellular K^+ concentrations were 5 and 140 mM.

of 6.0, 7.4, and 7.9. At pH_o 6.0, TASK-2 activity was barely enhanced by the intracellular alkalinization. Similar percent increases could be attained by shifting pH_i from 7.5 to 8.5 at permissive pH_o values of 7.4 and 7.9. Considering that half-maximum enhancement of current occurs at pH_o 8.03 (24), this result points to independence of the effects of intra- and extracellular pH on TASK-2.

Identification of a pH_i-sensing Residue Involved in the Gating of TASK-2 by Intracellular Protons—In contrast to the effect of pH_i in the TALK family, pH_o-gated channels TASK-1 and TASK-3 are largely insensitive to changes in pH_i. We verified this view using the acetate pH_i clamp approach described above, as shown in supplemental Fig. 2. To test whether the region of TASK-2 that confers the channel its pH_i sensitivity is situated in the rather large 260-amino acid C terminus, we constructed a chimera in which residues 243–502 of TASK-2 were replaced by the C-terminal residues 246–365 of the pH_i-insensitive TASK-3. This leaves a channel consisting of the putative membrane-resident part of TASK-2 and the intracellular C terminus tail of TASK-3 (Fig. 5). This construct, which we term 244TASK-2-245TASK-3, lacked pH_i sensitivity (supplemental Fig. 2), although it retained a near normal response to pH_o ($pK_{½}$ 9.06 ± 0.03, data not shown). This result suggests that pH_i sensitivity might reside in the C terminus. Ablation of all but the first 31 residues of the TASK-2 C terminus in the TASK-2Δ273 mutant did not alter the response to changes in pH_i (supplemental Fig. 2). Transplanting TASK-2 C terminus residues 244–502 of TASK-2 into a C terminus-less TASK-3 comprising residues 1–240 (Fig. 5) conferred TASK-3 some measure of pH_i dependence that was completely lacking in the TASK-3 WT construct (supplemental Fig. 2). These data suggested that if a single residue, or a short stretch of residues, acts as a pH_i sensor in TASK-2, it could be located in the region delimited by residues Val^{242} and Ser^{273}. Examination of such a region, which corresponds to the distal TM4 end and the beginning of the C-terminal segment, reveals various titratable lysine residues (see Fig. 5) that, given the approximate $pK_{½}$ of pH_i effect of ~8, might act as sensors. As seen in Fig. 5, neutralization of Lys^{454} and Lys^{258}, as well as a multiple neutralization of eight basic residues between Lys^{257} and Lys^{264}, did not alter pH_i dependence as tested by the NH_4Cl pulse approach. However, and as will be described in detail below, mutation at Lys^{245} had a profound effect on pH_i sensitivity as tested by the NH_4Cl pulse approach, which failed to elicit any change in current (data not shown).

Fig. 6*A* shows an experiment measuring the pH_i sensitivity of the TASK-2-K245A mutant. There was little evidence for significant effects of changes in pH_i. This is confirmed in the graph of Fig. 6*C* that reports average values for pH_i dependence of TASK-2-K245A and compares them with the response of WT TASK-2. Mutant TASK-2-K245C channels also lost all pH_i regulation. Mutation K245A in TASK-2 did not alter the general characteristics of the current, suggesting that Na^+/K^+ selectivity of TASK-2 were unaltered by removal of pH_i dependence (supplemental Fig. 1). Similarly, pH_o dependence was not altered by mutation K245A (supplemental Fig. 4).

Lys^{245} is located toward the C-terminal side of TM4 in TASK-2, a segment that plays the role of inner helix in these dimeric channels, and therefore lines the intracellular cavity of the pore. The other helix lining the intracellular cavity is TM2. As shown in Fig. 5, in addition to the conserved putative hinge Gly^{122} (Gly^{234} in TM4), there is not much sequence conservation between these two transmembrane domains. Nevertheless, there are some basic amino acids immediately following TM2 that were neutralized by mutation to test for their possible role in pH_i sensing. As reported in Fig. 5, none of these mutations affected the ability of intracellular alkalinization to activate TASK-2.

The effect of intracellular pH could also be detected in single channel recordings performed in inside-out patches from cells expressing TASK-2. The left-hand side of Fig. 7 shows traces of WT TASK-2 single channel activity in an inside-out patch exposed to intracellular pH values of 6.5, 7.5, and 8.5. As expected, the activity at acid pH was quite low, but openings occurred more frequently as the medium bathing the intracellular aspect of the membrane was alkalinized to pH 7.5 and 8.5. The calculated NP_o value increased from 0.03 at pH 6.5 to 0.41 and 0.72 at pH 7.5 and 8.5, respectively. The single channel conductance was not altered by changes in pH_i as can be seen in

```
A
TASK-3 numbering                    246                              274
TASK2/TASK3   229 LWIYL GLAWLSLFVN WRFLTMNSDE ERGEGEEGAA LPGNPSSVVT 270
TASK3/TASK2   226 MYILV GLTVIGAFLN WKVSMFVEVH KAIKKRRRRR KESFESSPHS 270
TASK-2 numbering                   244                              273

B
TASK-2        229 LWIYL GLAWLSLFVN WKVSMFVEVH KAIKKRRRRR KESFESSPHS 273
TASK-2-K254A      ----- ---------- ---------- A--------- ---------- (-)
TASK-2-K258A      ----- ---------- ---------- ----A----- ---------- (-)
TASK-2-KRs/As     ----- ---------- ---------- ---AAAAAAA A--------- (-)
TASK-2-K245A      ----- ---------- -A-------- ---------- ---------- (+)

C
TASK-2
TM4         203 TIGFGDFVAGVNPSANYHALYRYFVELWIYLGLAWLSLFVNWKVSMFVEVHKA
255
TM2          98 TIGYGNVAPKTPAG-------RLFCVFYGLFGVPLCLTWISALGKFFGGRAKR
143
TASK-2-K135A   ----------------------------------------------A--------- (-)
TASK-2-R140A   ----------------------------------------------A---- (-)
TASK-2-K142A   ----------------------------------------------A- (-)
TASK-2-R143A   ----------------------------------------------A (-)
```

FIGURE 5. **Search for a pH_i sensor controlling the gating of TASK-2.** *A*, chimaeras constructed from TASK-2 and TASK-3. The *borders* between segments of the two origins are depicted. Segments of TASK-2 origin are shaded in *gray*. *B*, portion of TASK-sequence containing TM4 and the putative glycine hinge (highlighted in *gray*). The *lines below* illustrate the functional result of mutagenesis done on this segment followed by (−), which indicates that the construct retained pH_i sensitivity, or (+) to indicate removal of intracellular pH dependence. *C*, portion of TASK-2 sequence containing TM4 and TM2 with their putative glycine hinges (highlighted in *gray*). The *lines below* illustrate the functional results of mutagenesis as in *B*.

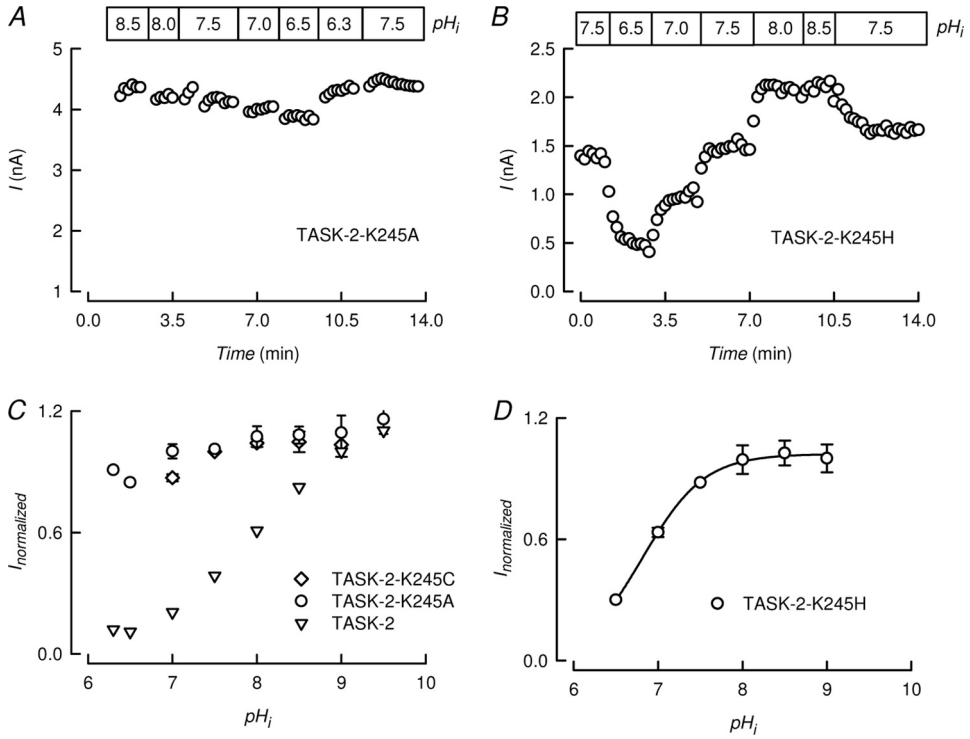

FIGURE 6. **Lysine 245 is a sensor that commands TASK-2 gating by intracellular pH.** *A* and *B*, time course of currents mediated by K245A and K245H mutants of TASK-2 recorded at 0 mV at various, indicated intracellular pH values. These experiments were performed exactly as described in the legend to Fig. 2*A*. *B*, pH_i dependence of TASK-2-K245A and TASK-2-K245C measured at 0 mV (means ± S.E., $n = 6$ and 3) is compared with that of WT TASK-2 that had been taken from Fig. 2*C* without *error bars*. *D*, pH_i dependence of TASK-2-K245H measured at 0 mV (means ± S.E., $n = 6$). Extracellular and intracellular K^+ concentrations were 5 and 140 mM, respectively in *A*–*D*.

activity of the TASK-2-K245A mutant. Mean values of NP_o for the mutant channels were 0.74 ± 0.08, 0.75 ± 0.02, and 0.79 ± 0.07 at intracellular pH values of 6.5, 7.5, and 8.5, respectively (means ± S.E., $n = 3$).

It might be expected that if Lys^{245} was a pH_i sensor in TASK-2, replacement by mutation to a different basic amino acid might preserve pH_i sensitivity but shift the activity pH_i curve according to the shift in pK_a of the amino acid. We have mutated Lys^{245} to His obtaining channels that generated currents sensitive to pH_i (Fig. 6*B*). As shown in Fig. 6*D*, TASK-2-K245H had a sensitivity to pH_i acid-shifted by >1 pH unit with respect to that of WT TASK-2 ($pK_{½}$ 6.8 ± 0.06, $n = 4$).

DISCUSSION

In contrast to what is seen with TASK-type K_{2P} potassium channels, we report here that TALK-type channels TASK-2 and TALK-2 are sensitive to pH_i, being activated by intracellular alkalinization and inhibited by intracellular acidification. We also present evidence that the control of gating by pH_i occurs by a separate mechanism than the well known regulation of TASK-2 by extracellular pH and that a lysine residue in the cytoplasmic end of TM4 acts as a pH_i sensor in the gating process.

Separate Mechanisms Mediate the Gating of TASK-2 Channels by Intra- and Extracellular pH—Although TASK-2 is gated open by intracellular alkalinization in a similar pH range as for extracellular alkalinization, several pieces of evidence suggest that the mechanism by which pH_i shifts are transduced into gating differs radically from that involved in pH_o gating. First, experiments designed to test the independence of pH_i and pH_o gating effects on TASK-2 showed that it was not possible to overcome closure by extracellular acidification by means of intracellular alkalinization, pointing to independent mechanisms for the effects of intra- and extracellular pH. Second, gating of TASK-2 by pH_o is mediated by arginine 224, so that mutant TASK-2-R224A

supplemental Fig. 3, which also reports mean values for NP_o as a function of pH_i. As shown in the right-hand panel of Fig. 7, there was no marked effect of varying intracellular pH on the

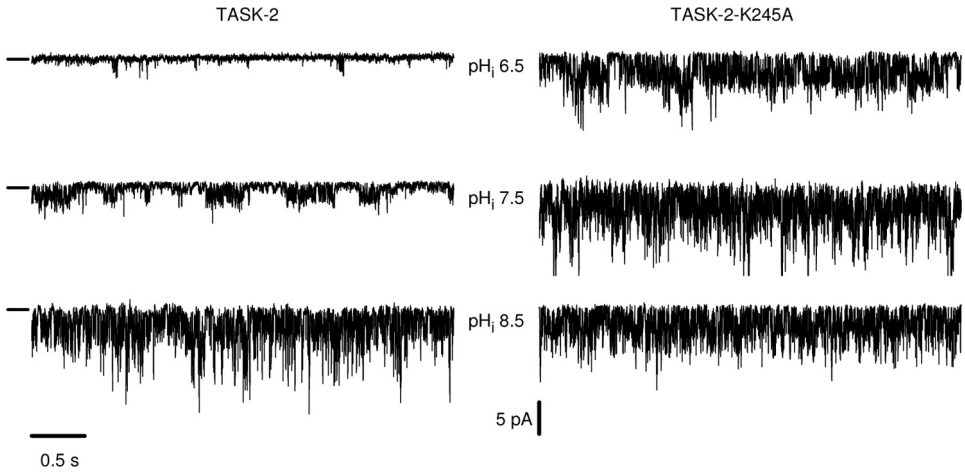

FIGURE 7. **Effect of mutation K245A on single channel activity of TASK-2 channels.** The pH$_i$ sensitivity of WT TASK-2 (*left*) and the mutant R245A (*right*) are shown at three different pH values of the bathing medium. The recording configuration was inside out, and the *short lines* at the *left* of the recordings show the closed channel levels. Openings are downward deflections and the patches illustrated contained at least three channels. The holding potential was −60 mV, and both pipette and bath solutions contained 140 mM K^+.

channels lack sensitivity to pH$_o$ (24). Despite being insensitive to changes in pH$_o$, however, TASK-2-R224A had a pH$_i$ dependence that was indistinguishable from that of WT TASK-2. Conversely, TASK-2-K245A, which is insensitive to pH$_i$, had a normal response to changes in pH$_o$. Third, pH$_o$-dependent gating is highly dependent upon extracellular K^+ concentration ($[K^+]_o$), so that increasing $[K^+]_o$ acid-shifts the pH$_o$ activity curve of TASK-2 and prevents full inhibition at acid pH$_o$. This contrasts with TASK-2 gating by pH$_i$, which was not affected by increasing $[K^+]_o$. Fourth, pH$_o$ modulation of TASK-2 is voltage-dependent with depolarization favoring the open channel state, whereas pH$_i$-gating of TASK-2 was not altered by membrane potential.

Location of the pH$_i$-controlled Gating Process in TASK-2—The molecular mechanisms by which of K^+ channel gating occurs has been widely studied functionally and also deduced from structural atomic level studies (26). Three forms of gating have been put forward. The first type was identified by comparing the structures of KcsA and MthK channels, crystallized under conditions that favor closed and open conformations, respectively (27, 28). The major difference between these crystal structures is in the position of the inner helices, which line the conduction pathway below the selectivity filter. In KcsA structure (the closed state), the four inner helices are straight and bundle together at the intracellular end to produce a narrow opening lined with hydrophobic amino acid residues, the hydrophobic seal (29), that restricts the movement of K^+ ions. In MthK, the inner helices are bent at a hinge point, a conserved glycine located roughly half way down the helix near the selectivity filter, creating a wide unimpeded pathway to ion passage. This type of gating is probably present in most K^+ channels, as suggested by the wide conservation of the glycine hinge (30) including channels of the K_{2P} family that have a glycine hinge in their TM2 and TM4 helices (31). Evidence for the presence of an intracellular gate has been recently obtained in the *Drosophila* KCNK0 K_{2P} channel (32). A second type of gating, first described as C-type inactivation (33), is sensitive to extracellular $[K^+]$ and mutations at residues near the external pore entrance and is thought to occur at the selectivity filter (26). C-type inactivation probably corresponds to the deformation of the selectivity filter of the KcsA channel that has been seen in channels crystallized with very low K^+ concentrations (34). It seems, therefore, that a decrease in occupancy of the selectivity filter by K^+ ions leads to its partial collapse with the carbonyl oxygens of the filter projecting obliquely rather than toward the central axis of the conduction pathway. Opening and closing of the *Drosophila* KCNK0 channel have been demonstrated to entail extracellular K^+ concentration-dependent C-type inactivation (35). A similar mechanism was proposed for gating by pH$_o$ of TASK-2 (24), TASK-1 (36), TREK-1 (10), and TREK-2 (11). A further type of gate mechanism, the ball-and-chain inactivation, has not been reported for K2P channels.

Activation of TASK-2 by extracellular alkalinization is mediated by neutralization of Arg^{224} located near the second pore domain (24) and involves changes in open probability (p_o) without affecting single channel conductance (2, 24, 37). It is thought that, in the protonated form, Arg^{224} decreases occupancy of the selectivity filter by K^+, thus creating a blocked state, a situation relieved by neutralization of Arg^{224} at alkaline pH$_o$ (24, 31). This gating at the selectivity filter, which might occur by the type of occupancy-related changes in pore structure revealed by molecular dynamic simulations (38), is highly dependent upon $[K^+]_o$, which is expected to counteract the filter collapse and therefore favor the open state. We show here that increasing the $[K^+]_o$ acid-shifted the pH$_o$ activity curve of TASK-2 and prevented full inhibition at acid pH$_o$. This characteristic of gating at the selectivity filter was absent from pH$_i$-dependent gating of TASK-2, which was not affected by increasing $[K^+]_o$. Another interesting characteristic of pH$_o$ modulation of TASK-2 is its voltage dependence with depolarization favoring the open channel state (2, 37). This finding, which we confirm here, could be interpreted as protons having to penetrate the transmembrane electric field to act on the channel sensor (4). However, the fact that the voltage dependence disappears when increasing $[K^+]_o$[3] suggests that an increased occupancy of a selectivity filter site(s) by K^+ as a consequence of depolarization, and therefore higher flux of K^+ from a side of high concentration, may be responsible for the effect. Such a model is similar to that proposed for the modulation of tetraethylammonium inhibition of Shaker channels coupled to the movement of K^+ ions within the selectivity filter (39, 40). At any rate, the lack voltage dependence of intracellular proton modulation of TASK-2 activity argues for a separate site for the pH$_i$-dependent gate. It is tempting to speculate that pH$_i$ gating is exerted by controlling inner helix bundle crossing in TASK-2, but we have no direct evidence for this. If this were

the case, it would appear that in contrast with what is seen in KCNK0 (32), the selectivity filter and inner gates of TASK-2 would open and close independently.

Lysine 245 Behaves as a pH_i-sensing Residue Mediating the Gating of TASK-2 by Intracellular Protons—In contrast to TASK-2 (and TALK-2), we found pH_o-gated channels TASK-1 and TASK-3 are largely insensitive to changes in pH_i. Through a chimeric channel approach utilizing the C-terminal region of TASK-3, we located the pH_i-sensing region in the C terminus of TASK-2. A C terminus truncation of TASK-2 further put the pH_i-sensing region within the first 31 residues of this region of TASK-2. Point mutations of various titratable residues in this stretch of C-terminal sequence led to the identification of Lys^{245} as a residue whose neutralization by mutation to A or C removed pH_i dependence from TASK-2.

The effect of Lys^{245} neutralization by mutation on the dependence of TASK-2 could be demonstrated in whole-cell and single channel recordings. Single channel open probability was increased by intracellular alkalinization in inside-out patches of membranes expressing WT TASK-2, without any effect on single channel conductance. The single channel activity of TASK-2-K245A was not dependent upon intracellular pH.

We predicted that if Lys^{245} was a pH_i sensor in TASK-2, its replacement by mutation to a different basic amino acid might preserve pH_i sensitivity but shift the activity pH_i curve according to the shift in pK_a of the amino acid. Comparison of the pH_i dependence of WT and TASK-2-K245H revealed that the mutation acid-shifted the $pK_{1/2}$ of the effect by >1 pH unit, consistent with Lys^{245} being a pH_i sensor in TASK-2.

Other K_{2P} channels whose gating is modulated by pH_i are TREK-1, TREK-2, and TRAAK. TREK-1 is a lipid-sensitive and mechano-gated channel of complex regulation, which is gated open by intracellular acidification (41). Glu^{306} in the proximal C-terminal domain has been demonstrated to be the proton sensor involved in this process (42). Membrane phospholipids open TREK-1 channels and a cluster of positively charged residues, which includes Glu^{306}, is the phospholipid-sensing domain. Protonation of Glu^{306} markedly enhances channel-phospholipid interaction, thus favoring the opening of TREK-1 (43). Intracellular pH also controls the gating of inwardly rectifying Kir channels, which are generally inhibited by intracellular acidification. No single residue has been found as yet to be responsible for pH_i gating in Kir channels. Lys^{80} of Kir1.1, a lysine residue located in the first transmembrane domain, was originally identified as the pH_i sensor (44), and an interaction with two distant arginine residues was proposed to be responsible for anomalous titration (45). More recent work has suggested, however, that Lys^{80} is not indispensable for pH_i-dependent gating of Kir channels (46, 47) and that it participates instead in highly conserved intrasubunit hydrogen bonding interactions between transmembrane domains that influence pH_i sensitivity indirectly (48). We explored the possibility that a similar mechanism might apply to Lys^{245} mediation of pH_i-dependent gating in TASK-2. Lys^{245} is located in TM4, and homology modeling suggested that it faces away from the pore and might approach Arg^{156} and Lys^{157} in TM3. The neutralization of Arg^{156} and Lys^{157} residues by mutation to alanine did not affect the action of pH_i on gating (data not shown). Clearly, further studies will be needed to determine the mechanism by which sensing of pH_i by lysine 245 leads to modulation of gating of TASK-2 and whether this affects the intracellular channel gate. Whatever the mechanistic details of the phenomenon reported, it is clear that a sensitive control of TASK-2 background K^+ channels by both extra- and intracellular pH implies that proton concentration could be the most important factor controlling membrane potential and K^+ recycling in the cells where it is expressed.

Acknowledgments—We are grateful to Drs. Jürgen Daut (Philipps-Universität, Marburg, Germany) and Donghee Kim (Rosalind Franklin University, Chicago, IL) for generously providing some of the cDNAs used in our experiments and to Robert W. Putnam (Wright State University, Dayton, OH) for advice on changing intracellular pH. F. Danilo González-Nilo and Valeria Márquez (Universidad de Talca, Chile) are gratefully acknowledged for insightful discussions concerning the structure of TASK-2. The Centro de Estudios Científicos (CECS) is funded by the Chilean Government through the Millennium Science Initiative and the Centers of Excellence Base Financing Program of Conicyt. Centro de Ingeniería de la Innovación asociado al CECS is funded by Conicyt and the Gobierno Regional de Los Ríos.

Addendum—Shortly after this paper was initially written, expression of TASK-2 was reported in the brainstem, including the retrotrapezoid nucleus. These TASK-2-positive cells were lost in Phox2b mutant mice that are a model for human congenital central hypoventilation syndrome (49). Retrotrapezoid nucleus neurons, whose development fails in Phox2b mutant mice, regulate breathing rate and intensity and active expiration and are therefore critical for the regulation of CO_2 (50). Sensing of CO_2 by retrotrapezoid nucleus neurons has been proposed to be via extra- or intracellular pH changes affecting background-type conductances that would regulate excitability. TASK-1 and TASK-3 K_{2P} channels were thought to be good candidates to mediate this signaling but have been discarded on the basis of experiments with double knock-out mice for these channels (51). Using a TASK-2 knock-out mouse, however, it is now shown that TASK-2 channels are important in mediating central CO_2 and O_2 chemosensitivity. Hypercapnia was shown to drive an acute ventilatory increase in WT but not in TASK-2-deficient mice (49). The authors hypothesize that active TASK-2 channels maintain a hyperpolarized condition of retrotrapezoid nucleus neurons, thus preventing a respiratory increase at low CO_2 (49). The strong ventilatory drive at high CO_2 could be the consequence of a decrease in TASK-2 channel activity. We think that the intracellular pH sensitivity of TASK-2 uncovered here could play a role in linking extracellular changes in CO_2 with intracellular pH changes and therefore TASK-2 activity. An understanding of the molecular mechanisms of this effect may contribute to the discovery of pharmacological strategies that attack central respiratory disorders.

REFERENCES

1. Goldstein, S. A., Bayliss, D. A., Kim, D., Lesage, F., Plant, L. D., and Rajan, S. (2005) *Pharmacol. Rev.* **57,** 527–540
2. Reyes, R., Duprat, F., Lesage, F., Fink, M., Salinas, M., Farman, N., and Lazdunski, M. (1998) *J. Biol. Chem.* **273,** 30863–30869
3. Kim, Y., Bang, H., and Kim, D. (2000) *J. Biol. Chem.* **275,** 9340–9347
4. Lopes, C. M., Zilberberg, N., and Goldstein, S. A. (2001) *J. Biol. Chem.* **276,** 24449–24452
5. Rajan, S., Wischmeyer, E., Xin, Liu, G., Preisig-Müller, R., Daut, J., Kar-

schin, A., and Derst, C. (2000) *J. Biol. Chem.* **275,** 16650–16657
6. Maingret, F., Patel, A. J., Lesage, F., Lazdunski, M., and Honoré, E. (1999) *J. Biol. Chem.* **274,** 26691–26696
7. Bang, H., Kim, Y., and Kim, D. (2000) *J. Biol. Chem.* **275,** 17412–17419
8. Lesage, F., Terrenoire, C., Romey, G., and Lazdunski, M. (2000) *J. Biol. Chem.* **275,** 28398–28405
9. Kim, Y., Bang, H., Gnatenco, C., and Kim, D. (2001) *Pflugers Arch.* **442,** 64–72
10. Cohen, A., Ben-Abu, Y., Hen, S., and Zilberberg, N. (2008) *J. Biol. Chem.* **283,** 19448–19455
11. Sandoz, G., Douguet, D., Chatelain, F., Lazdunski, M., and Lesage, F. (2009) *Proc. Natl. Acad. Sci. U.S.A.* **106,** 14628–14633
12. Hebert, S. C., Desir, G., Giebisch, G., and Wang, W. (2005) *Physiol. Rev.* **85,** 319–371
13. Heitzmann, D., and Warth, R. (2008) *Physiol. Rev.* **88,** 1119–1182
14. Warth, R., Barrière, H., Meneton, P., Bloch, M., Thomas, J., Tauc, M., Heitzmann, D., Romeo, E., Verrey, F., Mengual, R., Guy, N., Bendahhou, S., Lesage, F., Poujeol, P., and Barhanin, J. (2004) *Proc. Natl. Acad. Sci. U.S.A.* **101,** 8215–8220
15. Boron, W. F. (2006) *J. Am. Soc. Nephrol.* **17,** 2368–2382
16. Niemeyer, M. I., Cid, L. P., Barros, L. F., and Sepúlveda, F. V. (2001) *J. Biol. Chem.* **276,** 43166–43174
17. Cid, L. P., Niemeyer, M. I., Ramírez, A., and Sepúlveda, F. V. (2000) *Am. J. Physiol. Cell Physiol.* **279,** C1198–1210
18. Yon, J., and Fried, M. (1989) *Nucleic Acids Res.* **17,** 4895
19. Grinstein, S., Romanek, R., and Rotstein, O. D. (1994) *Am. J. Physiol.* **267,** C1152–C1159
20. Yuan, Y., Shimura, M., and Hughes, B. A. (2003) *J. Physiol.* **549,** 429–438
21. Hartzler, L. K., Dean, J. B., and Putnam, R. W. (2008) *Adv. Exp. Med. Biol.* **605,** 333–337
22. Roos, A., and Boron, W. F. (1981) *Physiol. Rev.* **61,** 296–434
23. Duprat, F., Lesage, F., Fink, M., Reyes, R., Heurteaux, C., and Lazdunski, M. (1997) *EMBO J.* **16,** 5464–5471
24. Niemeyer, M. I., González-Nilo, F. D., Zúñiga, L., González, W., Cid, L. P., and Sepúlveda, F. V. (2007) *Proc. Natl. Acad. Sci. U.S.A.* **104,** 666–671
25. Cohen, A., Ben-Abu, Y., and Zilberberg, N. (2009) *Eur. Biophys. J.* **39,** 61–73
26. Yellen, G. (2002) *Nature* **419,** 35–42
27. Doyle, D. A., Morais Cabral, J., Pfuetzner, R. A., Kuo, A., Gulbis, J. M., Cohen, S. L., Chait, B. T., and MacKinnon, R. (1998) *Science* **280,** 69–77
28. Jiang, Y., Lee, A., Chen, J., Cadene, M., Chait, B. T., and MacKinnon, R. (2002) *Nature* **417,** 515–522
29. Armstrong, C. M. (2003) *Sci. STKE.* **2003,** re10
30. Magidovich, E., and Yifrach, O. (2004) *Biochemistry* **43,** 13242–13247
31. Niemeyer, M. I., González-Nilo, F. D., Zúñiga, L., González, W., Cid, L. P., and Sepúlveda, F. V. (2006) *Biochem. Soc. Trans.* **34,** 899–902
32. Ben-Abu, Y., Zhou, Y., Zilberberg, N., and Yifrach, O. (2009) *Nat. Struct. Mol. Biol.* **16,** 71–79
33. Hoshi, T., Zagotta, W. N., and Aldrich, R. W. (1991) *Neuron* **7,** 547–556
34. Zhou, Y., Morais-Cabral, J. H., Kaufman, A., and MacKinnon, R. (2001) *Nature* **414,** 43–48
35. Zilberberg, N., Ilan, N., and Goldstein, S. A. (2001) *Neuron* **32,** 635–648
36. Stansfeld, P. J., Grottesi, A., Sands, Z. A., Sansom, M. S., Gedeck, P., Gosling, M., Cox, B., Stanfield, P. R., Mitcheson, J. S., and Sutcliffe, M. J. (2008) *Biochemistry* **47,** 7414–7422
37. Kang, D., and Kim, D. (2004) *Biochem. Biophys. Res. Commun.* **315,** 836–844
38. Bernèche, S., and Roux, B. (2005) *Structure* **13,** 591–600
39. Thompson, J., and Begenisich, T. (2003) *J. Gen. Physiol.* **122,** 239–246
40. Thompson, J., and Begenisich, T. (2005) *J. Gen. Physiol.* **125,** 619–629
41. Dedman, A., Sharif-Naeini, R., Folgering, J. H., Duprat, F., Patel, A., and Honoré, E. (2009) *Eur. Biophys. J.* **38,** 293–303
42. Honoré, E., Maingret, F., Lazdunski, M., and Patel, A. J. (2002) *EMBO J.* **21,** 2968–2976
43. Chemin, J., Patel, A. J., Duprat, F., Lauritzen, I., Lazdunski, M., and Honoré, E. (2005) *EMBO J.* **24,** 44–53
44. Fakler, B., Schultz, J. H., Yang, J., Schulte, U., Brandle, U., Zenner, H. P., Jan, L. Y., and Ruppersberg, J. P. (1996) *EMBO J.* **15,** 4093–4099
45. Schulte, U., Hahn, H., Konrad, M., Jeck, N., Derst, C., Wild, K., Weidemann, S., Ruppersberg, J. P., Fakler, B., and Ludwig, J. (1999) *Proc. Natl. Acad. Sci. U.S.A.* **96,** 15298–15303
46. Leng, Q., MacGregor, G. G., Dong, K., Giebisch, G., and Hebert, S. C. (2006) *Proc. Natl. Acad. Sci. U.S.A.* **103,** 1982–1987
47. Rapedius, M., Haider, S., Browne, K. F., Shang, L., Sansom, M. S., Baukrowitz, T., and Tucker, S. J. (2006) *EMBO Rep.* **7,** 611–616
48. Rapedius, M., Fowler, P. W., Shang, L., Sansom, M. S., Tucker, S. J., and Baukrowitz, T. (2007) *Neuron* **55,** 602–614
49. Gestreau, C., Heitzmann, D., Thomas, J., Dubreuil, V., Bandulik, S., Reichold, M., Bendahhou, S., Pierson, P., Sterner, C., Peyronnet-Roux, J., Benfriha, C., Tegtmeier, I., Ehnes, H., Georgieff, M., Lesage, F., Brunet, J. F., Goridis, C., Warth, R., and Barhanin, J. (2010) *Proc. Natl. Acad. Sci. U.S.A.* **107,** 2325–2330
50. Guyenet, P. G., and Mulkey, D. K. (2010) *Respir. Physiol. Neurobiol.*, in press
51. Mulkey, D. K., Talley, E. M., Stornetta, R. L., Siegel, A. R., West, G. H., Chen, X., Sen, N., Mistry, A. M., Guyenet, P. G., and Bayliss, D. A. (2007) *J. Neurosci.* **27,** 14049–14058